Linhoff, B.S., and Lunzer, J.J., 2021, Discovery of a large subsoil nitrate reservoir in an arroyo floodplain and associated aquifer contamination: Geology, v. 49, https://doi.org/10.1130/G47916.1

Discovery of a large subsoil nitrate reservoir in an arroyo floodplain and associated aquifer contamination

Benjamin S. Linhoff[1] and John J. Lunzer[1]

[1]U.S. Geological Survey, New Mexico Water Science Center, 6700 Edith Blvd NE, Albuquerque, NM 87113

SUPPLEMENTAL MATERIAL

Tijeras Arroyo

A U.S. Geological Survey (USGS) streamgage site (USGS Site ID: 08330600) on Tijeras Arroyo located 8 km downstream from the field area recorded flow events between 3 and 91 days per year during 1983–2019 (U.S. Geological Survey, 2020). During this time, monsoon season streamflows during rain events were typically 1–3 m^3/s. Past research has shown that near the mountain front, flow through Tijeras Arroyo has decreased approximately 10-fold since the 1940s likely due to increased development in the watershed (Anderholm, 2000; Plummer et al., 2012).

Groundwater sampling

In 2017, the USGS collected groundwater samples through a Teflon sampling line at or near the well head using a submersible Bennett Pump. Prior to and after using the Bennett Pump, the pump was cleaned using a sequence of 0.2 % Liquinox soap, tap water, 18 megaohm deionized water, methanol, and finally 18 megaohm certified organic free deionized water (U.S. Geological Survey, variously dated). The pump was placed in the middle of the well's screened interval and pumped at approximately 1 gallon/minute. Groundwater level was monitored during purging to ensure good communication with the aquifer during pumping. Sampling began after at least one well volume was purged and at least five subsequent measurements of pH, temperature, specific conductivity (SC), turbidity, and dissolved oxygen (O_2) collected 5 minutes apart were within ±0.1 pH units, ±0.2°C for temperature, ±5% for SC <100 µS/cm and ±3% for SC>100 µS/cm, ±0.3 mg/L for O_2, and ±10% for turbidity <100 NTU.

All samples were stored at 4°C until extraction. Nutrient samples were filtered to 0.45 µm and collected in 125-mL brown polyethylene bottles before being analyzed within 30 days of collection using methods outlined in Fishman (1993) and Patton and Kryskalla (2011). Major anions and cations were measured to ensure charge balance of <5%. Samples collected for major cations were filtered to 0.45 µm, acidified to pH<2, and stored chilled until analysis. Major anion samples were filtered to 0.45 µm, chilled until analysis. Methods for analyzing major ions are described in Fishman (1993). Carbonate species (H_2CO_3, HCO_3^-, and CO_3^{2-}) were calculated from field alkalinity titrations. All nutrient and major element analyses for the 2017 field campaign were completed at the USGS National Water Quality Laboratory in Denver, Colorado. All data collected at the sites in 2017 by USGS are available from the USGS National Water Information System (NWIS) database (U.S. Geological Survey, 2020b) using the USGS site ID numbers given in Tables S1 and S2.

Results from the USGS sampling campaign were compared to time series data collected and analyzed using similar methods by the U.S. Air Force Civil Engineer Center. These time series data were retrieved from the Environmental Program Info Management System (ERPIMS) database and are shown in Tables S1 and S2. More information about the U.S. Air Force ERPIMS database can be found here:

https://www.afcec.af.mil/What-We-Do/Environment/Restoration/ERPIMS.aspx.

Sediment core sampling

Sediment samples were collected at eight sites using a track mounted Geoprobe® dual tube hollow-stem auguring system without drilling fluids. Using this system, an outer drive casing was advanced incrementally with hammer percussion into the ground with an inner rod string cycled in and out of the casing to retrieve subsoil cores. Cores were retrieved to 15 m or until drilling met refusal. Cores were collected in August and flow in Tijeras Arroyo was observed following several storms including the day prior to sampling AC.

Cores were collected in 152-cm long, 3.3-cm inner diameter plastic sleeves. These were sealed immediately using caps, electrical tape, and parafilm, and placed on ice in the shade to minimize evaporation. Extracted cores were sampled in ~30 cm intervals and examined for gravimetric water content and dry and wet bulk density following methods from Grossman and Reinsch (2002). Lithology was recorded through each subsoil profile (S3 Observed Soil Types). Porosity was calculated from dry bulk density assuming a particle density of silicates (2.3 g/cm^3). Sediment water potential was measured at 0.3-m intervals using a WP4C benchtop instrument from Meter Environment. Water potential was subsequently converted from pressure (MPa) to hydraulic head (m). Environmentally mobile anions in the unsaturated zone were determined from 18 hour 1:20 sediment to water extractions using 18 megaohm deionized water. Extractions were measured for Cl, NO_3, NO_2, SO_4, and Br concentrations using ion chromatography; porewater concentrations were determined from the anion mass mobilized during the 18 megaohm deionized water extraction and the gravimetric water content of each sample. Sediment porewater concentrations, matric potential, and moisture content are in Table S3 and in the NWIS database (U.S. Geological Survey, 2020b) using the USGS site ID numbers given in Table 3.

Subsoil sediment types

Soil profile data was obtained from field records taken during coring and lab analysis performed on field samples. These results were used to determine the proper soil properties for use in the Hydrus model. Figure S1 and Table S4 below show the lab determined soil profiles for each of the relevant sites as well as raw results obtained from lab analysis.

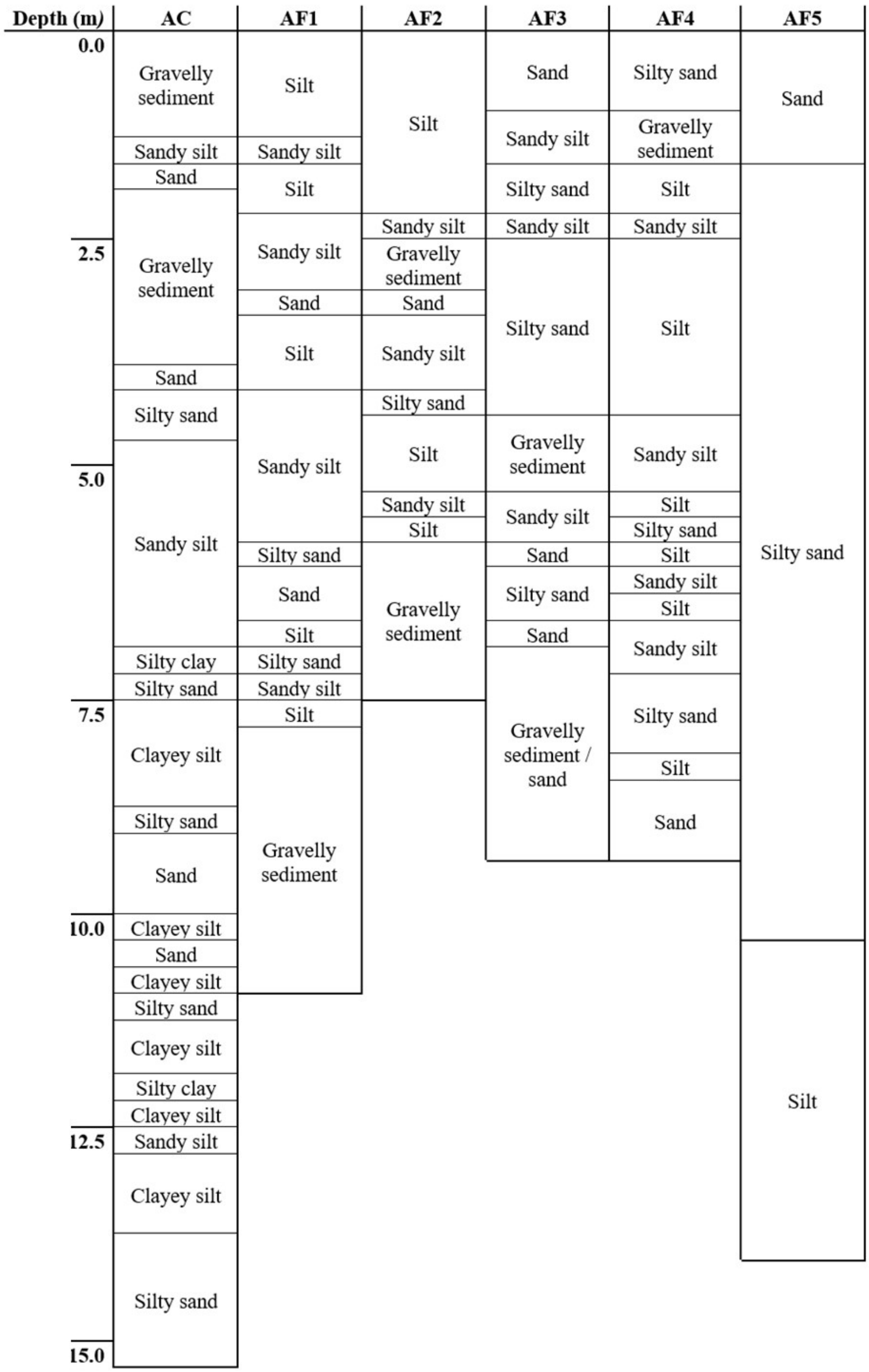

Figure S1. Lab determined subsoil profiles for arroyo channel and arroyo floodplain sites.

Table S4. Lab determined subsoil composition, water content, dry bulk density, and porosity.

Soil type	Composition	Water content range (g)	Dry bulk density range (g/cm^3)	Porosity range (%)
Gravelly sediment	15–60% gravel	0.9–3.7	1.4–2.2	21.1–48.1
Sand	90–100% sand, 0–10% silt	0.7–15.8	1.2–1.8	33.2–53.8
Silty sand	60–85% sand, 15–40% silt	0.6–16.3	0.9–1.9	26.9–65.9
Sandy silt	60–90% silt, 10–40% sand	1.6–12.7	1.0–1.9	28.1–59.4
Silty sand	90–100% silt, 0–10% sand	1.7–6.5	0.9–1.5	41.8–66.0
Clayey silt	70–80% silt, 20–30% clay	12.2–19.7	1.4–1.6	34.6–47.4
Silty clay	50–60% clay, 40–50% silt	15.9–20.8	1.4–1.6	39.2–46.4

Plant species

The dominant plant species identified near coring sites in the arroyo floodplain (AF1–AF5) were *Atriplex canescens* (fourwing saltbrush), *Glossopetalon spinescens* (spiny greasebrush), *Tetradymia* (horsebrush), and various tussock grasses. Several *Elaeagnus angustifolia* trees (Russian olive) were also found at the arroyo channel edge. Many of these species can produce tap roots to 8–10-m depth (Conrad, 1987); however, no roots were encountered in any of the core samples. Vegetation near the mesa sites (M1 and M2) was primarily short (~0.2 m) tussock grasses interspersed with small (0.2 m) *Atriplex canescens*, *Salsola kali* (Russian thistle), and *Gutierrezia* (snakeweed).

Water matric potential

Water potential profiles were similar between the arroyo floodplain and mesa top sites while water potential near zero in the arroyo channel implies near saturation (Table S3). Representative profiles were selected to show a typical water potential profile for channel, floodplain, and mesa top sites (Figure S2). The vadose zone model assumed the water matric potential was 0 m within the channel and -500 m in the arroyo floodplain based off these water potential profiles.

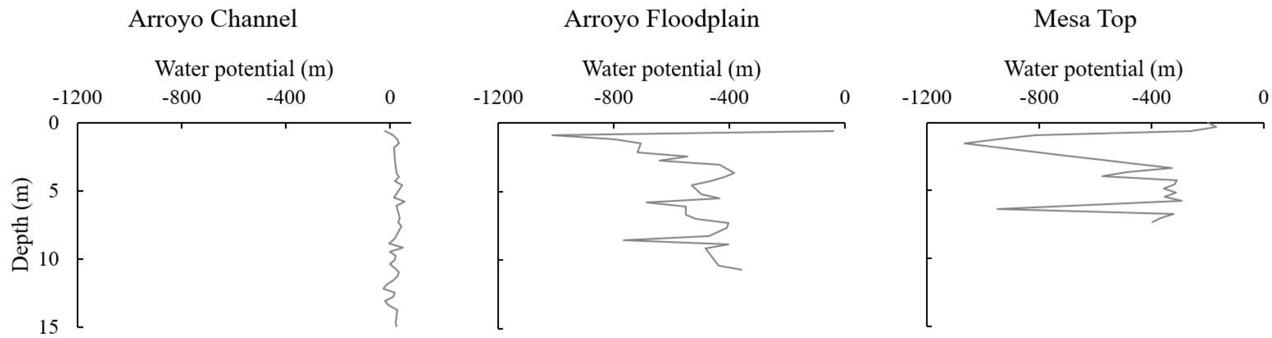

Figure S2. Representative water potential profiles for arroyo channel, arroyo floodplain and mesa top sites.

Chloride mass balance calculation

Subsoil zone chloride (Cl) profiles in the mesa sites show a profile typical of the desert southwestern United States with a “Cl bulge” in the top 10 m of the profile. The lower concentrations of Cl below the Cl bulge are generally interpreted to be the result of pluvial conditions during the Pleistocene (>12–15 Ka) and periods of past aquifer recharge (Phillips, 1994). The Cl bulges form as the result of evaporation and plant uptake of precipitation in the upper 10 m of the subsoil profile and indicate zero recharge and an upward potential gradient for water movement (Walvoord et al., 2004).

Downward displacement of Cl bulges is the result of incomplete flushing during flooding (Walvoord et al., 2003; Scanlon et al., 2008). Two distinct Cl and NO_3 bulges were observed in sites AF1, AF4, and AF5 likely indicating past partial flushing of solutes from subsoils to deeper depths during flooding events in the Tijeras Arroyo floodplain. Chloride mass balance (CMB) age calculations indicate these flushing events occurred 4,500 ybp, 1,800 ybp, and 600 ybp for sites AF1, AF4, and AF5, respectively (Table S3). The discrepancy between these ages and the lack of multiple Cl bulges at sites AF2 and AF3 may imply multiple flooding events that did not cover the entire floodplain. Alternatively, these lower bulges may be the result of lateral transport of solutes from beneath the arroyo channel to the surrounding floodplain. Hence CMB age calculations in the arroyo floodplain are difficult to interpret.

Assuming one-dimensional piston flow and constant Cl deposition, Cl residence time can be calculated by dividing the Cl inventory by the annual Cl deposition:

$$t_z = \frac{\int_0^z \theta C_{Cl} dz}{D_z}$$

where t_z is the CMB age to depth z, θ is the volumetric water content (L^3 L^{-3}), C_{Cl} is the Cl inventory, and D_z is the atmospheric Cl depositional flux. We estimated the Cl depositional flux from two nearby stations (NM07 and NM09) of the National Atmospheric Depositional Program (NADP, 2019) from the mean annual deposition rate spanning 1982–2000 at NM09 and 1982–2018 for NM07. Because these stations receive mean rainfall (36 cm and 31 cm, respectively) greater than the study area (23 cm), we scaled the estimated Cl depositional flux from 0.3 kg/ha (mean of NM07 and NM09) to 0.2 kg/ha.

Table S5. The nitrate (NO_3) inventory was estimated using the entire sample depth. The total CMB age is the apparent CMB age of the entire sample column. The apparent NO_3 flux was calculated using the NO_3 inventory and the total apparent CMB age. Mean atmospheric NO_3 deposition was 1.27 kg $ha^{-1}y^{-1}$.

Site name	NO_3 inventory (kg ha^{-1})	CMB age at 5 m (ybp)	Total CMB age (ybp)	Apparent NO_3 flux (kg ha^{-1} yr^{-1})
AF1	18000	8600	12000	1.5
AF2	17000	5200	6400	2.7
AF3	9800	6600	10000	0.98
AF4	12000	5300	7900	1.5
AF5	38000	2600	15000	2.5
MT1	59	17000	17000	0.0035
MT2	95	13000	22000	0.0043
AC	210			

Vadose Zone Model

Hydrus 1-D (Šimůnek et al., 2012) is a one-dimensional finite element model that simulates the flow of water through variably saturated media by numerically solving Richards' equation (Richards, 1931). The model accounted for observed changes in lithology with depth, and measured sediment moisture content and water potential (Figure S1 and Table S3). The domain was horizontally orientated and 15 m long—the distance between the channel and the nearest field measurement of subsoil water potential (AF4 to AC). The model domain was bounded by two constant pressure head boundaries of 0 m and -500 m, representative of the arroyo channel and floodplain sites (Figure S2). Based on streamgage observations of flow in the Tijeras Arroyo channel (USGS Site ID: 08330600, U.S. Geological Survey, 2020a), we estimated a range of annual days saturation beneath the arroyo of 60–100 days.

Sediment types from the subsoil profiles were paired with the appropriate U.S. Department of Agriculture sediment textural class (Soil Survey Staff, 1999). Using these classes, Hydrus 1-D provided default van Genuchten-Mualem sediment hydraulic properties were chosen for each sediment type. Gravelly sediments were grouped with sands to maintain the conservative nature of the Hydrus 1-D model.

Model results estimated that 364,000–948,000 m^3 y^{-1} of water moves from beneath the arroyo channel into the adjacent unsaturated zone. Previous estimates of infiltration through Tijeras Arroyo have ranged from 600,000–2,400,000 m^3 y^{-1} (Anderholm, 2000; Sanford et al., 2000), hence our model indicates 15–100 % of water infiltrating Tijeras Arroyo is lost in the thick unsaturated zone.

Table S6. The hydraulic soil properties used for each textural class and the default van-Genuchten-Mualem soil hydraulic properties based off soil textural classification.

Soil name	Observed soil	Ks (m/day)	Residual water content	Saturated water content	Alpha	n
Coarse (sand)	Gravelly sediment/sand	7.128	0.045	0.4	14.5	2.68
Loamy sand	Silty sand	3.502	0.057	0.41	12.4	2.28
Sandy loam	Sandy silt	1.061	0.065	0.41	7.5	1.89
Silt	Silt	0.06	0.034	0.46	1.6	1.37

The modeling process followed a specific workflow between Hydrus 1-D and Microsoft Excel. Figure S3 depicts a flow chart describing the process from Hydrus 1-D inputs and outputs to Excel inputs and outputs. Fixed inputs of pressure head boundaries (0 m and -500 m), time discretization, and domain dimensions (Table S6) were initially entered in Hydrus 1-D. Then the days of saturation were manipulated in Hydrus 1-D by changing the model duration (60–100 days). Finally, specific sediment input parameters (Table S6) for the different sediment types were entered in Hydrus 1-D. This was performed running multiple models until a cumulative flux of water into the vadose zone was determined for each sediment type and various days of saturation.

Hydrus 1-D obtained cumulative flux values were then moved into Microsoft Excel and applied as a variable input. A range of cumulative fluxes were applied to the corresponding sediment type within the profile. This cumulative flux for a specific sediment type was multiplied by the thickness of that sediment type within the profile. Once a cumulative flux was determined for a thickness of each sediment type in a profile, the fluxes were summed to produce a total cumulative flux per unit channel length into that particular arroyo floodplain site.

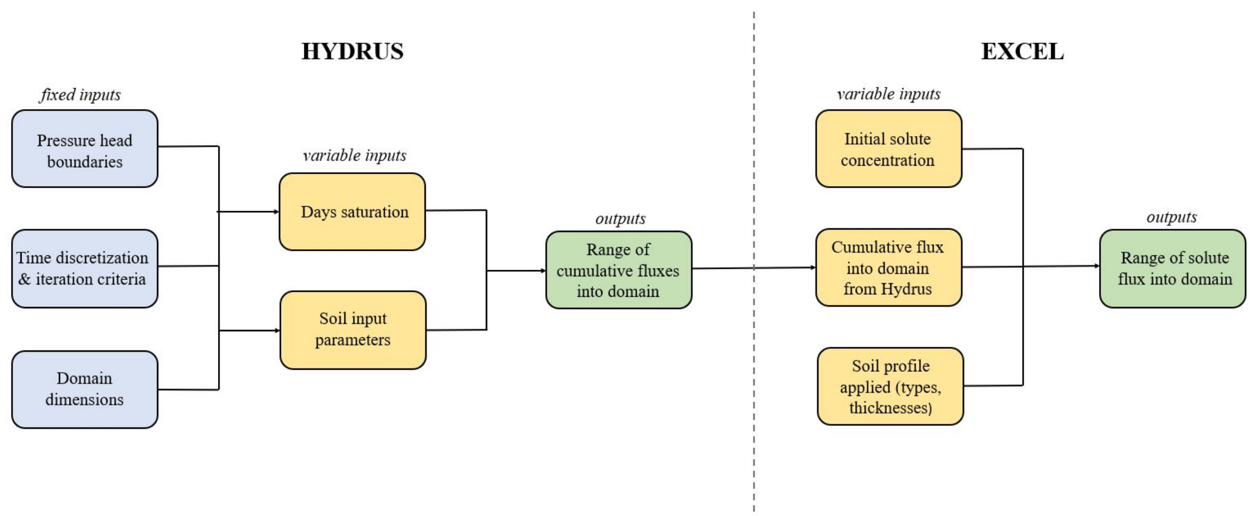

Figure S3. Flow diagram depicting the inputs, outputs, and workflow between Hydrus and Microsoft Excel. Fixed inputs are shown in blue, variable inputs are shown in yellow and outputs are shown in green.

Total Volume Calculations

In order to determine the approximate amount of water predicted to be leaving the saturated channel sediments and entering the vadose zone throughout the entire arroyo system, several key assumptions were made. The channel with corresponding floodplain was measured using satellite imagery to be approximately 19 km in length. Furthermore, other works indicate the relatively high water matric potential gradient typically exists no greater than 20 m depth before the magnitude of the gradient decreases rapidly (Walvoord et al., 2003). Using these geometries and the calculated total cumulative fluxes per subsoil profile, a range of volumes of water moving from the arroyo channel sediments to the floodplain sediments was determined. This final volume of water was multiplied by two to account for the relation existing on both sides of the channel.

Solute mass flux calculations

Once water fluxes were modeled, the Cl mass flux into the floodplain sediments from lateral unsaturated flow was determined to estimate solute accumulation time. Using porewater Cl concentrations at site AC (10–20 mg/L; Figure 2) as initial concentrations, saturated arroyo sediments could convey between 0.13–0.70 kg yr^{-1} of Cl per meter channel length into the unsaturated floodplain sediments. As the arroyo channel length is ~19 km, this resulted in a Cl flux of 2,400–13,300 kg Cl yr^{-1} to the floodplain. Given a floodplain size of ~800 ha (estimated from a digital elevation model and satellite imagery), and assuming Cl inventories across the floodplain similar to our observations, Cl inventories in the floodplain could be reached within 200–800 years—eight to 75 times faster than atmospheric deposition CMB calculations (Table S4). The estimated range in the accumulation time and Cl flux accounts for a range in each input parameters.

Sediments beneath the arroyo channel had slightly positive (saturated) pressure. To make our model more conservative, we assumed zero pressure through the channel sediments. Furthermore, time varying saturation was handled by stopping the model after the specified days of saturation and not letting the sediments drain. This made the lateral flux estimate an underestimation as a slow flux will occur when sediments are not saturated. However, using conservative estimates is useful in providing more confidence in our hypothesis—that seasonal water flow through the arroyo could lead to large solute build up in the subsoil of the arroyo floodplain.

Precipitation accumulation

Accumulation rates of Cl in the entire floodplain were determined by taking the reported atmospheric rate for the region (NADP, 2019) and multiplying it by the entire floodplain area. The entire floodplain area was measured based off topography and determined to be roughly 800 ha. This accumulation rate was then compared to observed pore water concentrations to determine an estimated time for the observed Cl concentrations to accumulate if atmospheric deposition is the only solute input.

Figure S4. Satellite images of Tijeras Arroyo taken in 2004 and 2018. The 2004 channel is shown in blue in the lower image. In the 14 years between the images, the Tijeras Arroyo Channel has moved ~1 m/y at the bends. Site AF2 is shown in the lower left side of the images. Also shown is the increase in plant cover from 2004–2018. Base map data from Google, 2020.

Supplemental Material Citations:

Anderholm, S.K., 2000, Mountain-front recharge along the eastern side of the Middle Rio Grande Basin, central New Mexico, in U.S. Geological Survey Middle Rio Grande Basin Study Proceedings of the Second Annual Workshop, Albuquerque, New Mexico, February 10-11,1998, Citeseer, p. 66–69.

Conrad, C.E., 1987, Common shrubs of chaparral and associated ecosystems of southern

California: US Department of Agriculture, Forest Service, Pacific Southwest Forest and~…, v. 99.

Grossman, R.B., and Reinsch, T.G., 2002, Bulk density and linear extensibility, in Methods of soil analysis: Part 4 physical methods, Wiley Online Library, v. 5, p. 201–228.

Fishman, M.J., 1993, Methods of analysis by the US Geological Survey National Water Quality Laboratory: Determination of inorganic and organic constituents in water and fluvial sediments: US Department of the Interior, US Geological Survey.

National Atmospheric Deposition Program (NADP), 2019, data available on the World Wide Web, accessed [November 3, 2019], at [http://nadp.slh.wisc.edu/data/sites/siteDetails.aspx?net=NTN&id=NM07].

Patton, C.J., and Kryskalla, J.R., 2011, Colorimetric determination of nitrate plus nitrite in water by enzymatic reduction, automated discrete analyzer methods: US Geological Survey Techniques and Methods, v. 34.

Phillips, F.M., 1994, Environmental tracers for water movement in desert soils of the American southwest: Soil Science Society of America Journal, v. 58, p. 15–24, doi:10.2136/sssaj1994.03615995005800010003x.

Plummer, N., Bexfield, L.M., Anderholm, S.K., Sanford, W.E., and Busenberg, E., 2012, Geochemical characterization of ground-water flow in the Santa Fe group aquifer system , Middle Rio Grande Basin , New Mexico: U.S.G.S. Water-Resources Investigations Report 03-4131, p. 1–395.

Richards, L.A., 1931, Capillary conduction of liquids through porous mediums: Physics, v. 1, p.

318–333.

Sanford, W.E., Plummer, L.N., McAda, D.P., Bexfield, L.M., and Anderholm, S.K., 2000, Estimation of hydrologic parameters for the ground-water model of the Middle Rio Grande Basin using carbon-14 and water-level data: US Geological Survey Open-file Report, p. 4–6.

Scanlon, B., Reedy, R., and Bronson, K., 2008, Impacts of Land Use Change on Nitrogen Cycling Archived in Semiarid Unsaturated Zone Nitrate Profiles, Southern High Plains, Texas: Environmental Science & Technology, v. 42, doi:10.1021/es800792w.

Šimůnek, J., van Genuchten, M. Th., and Šejna, M., 2012, HYDRUS: Model use, calibration and validation, Special issue on Standard/Engineering Procedures for Model Calibration and Validation, Transactions of the ASABE, v. 55, p. 1261-1274, 2012.

Soil Survey Staff. 1999. Soil taxonomy: A basic system of soil classification for making and interpreting soil surveys. 2nd edition. Natural Resources Conservation Service. U.S. Department of Agriculture Handbook p. 436.

U.S. Geological Survey, 2020a, USGS 08330600 TIJERAS ARROYO NR ALBUQUERQUE, NM *in* USGS Water Data for the Nation, accessed [January 10, 2020], at https://doi.org/10.5066/F7P55KJN. [Site information directly accessible at https://waterdata.usgs.gov/nwis/inventory?agency_code=USGS&site_no=08330600].

U.S. Geological Survey, 2020b, USGS water data for the Nation: U.S. Geological Survey National Water Information System database, accessed [January 20, 2020] at https://doi.org/10.5066/F7P55KJN.

Walvoord, M.A., and Phillips, F.M., 2004, Identifying areas of basin-floor recharge in the Trans-Pecos region and the link to vegetation: v. 292, p. 59–74, doi:10.1016/j.jhydrol.2003.12.029.

Walvoord, M.A., Phillips, F.M., Stonestrom, D.A., Evans, R.D., Hartsough, P.C., Newman, B.D., and Striegl, R.G., 2003, A Reservoir of Nitrate Beneath Desert Soils: Science, v. 302, doi:10.1126/science.1086435.

U.S. Geological Survey (USGS), variously dated, National field manual for the collection of water-quality data: U.S. Geological Survey Techniques of Water-Resources Investigations, book 9, chaps. A1-A10, available online at http://pubs.water.usgs.gov/twri9A.